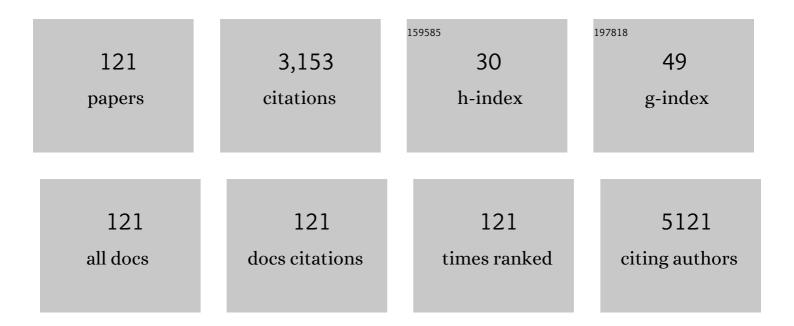
## Suklyun Hong

List of Publications by Year in descending order

Source: https://exaly.com/author-pdf/720071/publications.pdf Version: 2024-02-01



#	Article	IF	CITATIONS
1	Computational Study of Hydrogen Storage Characteristics of Covalent-Bonded Graphenes. Journal of the American Chemical Society, 2007, 129, 8999-9003.	13.7	161
2	Systematic study of electronic structure and band alignment of monolayer transition metal dichalcogenides in Van der Waals heterostructures. 2D Materials, 2017, 4, 015026.	4.4	160
3	Charge Mediated Reversible Metal–Insulator Transition in Monolayer MoTe <sub>2</sub> and W <sub><i>x</i></sub> Mo <sub>1–<i>x</i></sub> Te <sub>2</sub> Alloy. ACS Nano, 2016, 10, 7370-7375.	14.6	133
4	Nanocrystalline Graphite Growth on Sapphire by Carbon Molecular Beam Epitaxy. Journal of Physical Chemistry C, 2011, 115, 4491-4494.	3.1	113
5	Modification of Electrical Properties of Graphene by Substrate-Induced Nanomodulation. Nano Letters, 2013, 13, 3494-3500.	9.1	94
6	Phase stability and elastic moduli of Cr2Nb by first-principles calculations. Intermetallics, 1999, 7, 5-9.	3.9	93
7	In situ hybridization of carbon nanotubes with bacterial cellulose for three-dimensional hybrid bioscaffolds. Biomaterials, 2015, 58, 93-102.	11.4	82
8	Remote heteroepitaxy of GaN microrod heterostructures for deformable light-emitting diodes and wafer recycle. Science Advances, 2020, 6, eaaz5180.	10.3	80
9	Structure of the Ba-InducedSi(111)-(3×2)Reconstruction. Physical Review Letters, 2001, 87, 056104.	7.8	64
10	Ab initio study of the effect of water adsorption on the carbon nanotube field-effect transistor. Applied Physics Letters, 2006, 89, 243110.	3.3	63
11	Atomic-scale dynamics of triangular hole growth in monolayer hexagonal boron nitride under electron irradiation. Nanoscale, 2015, 7, 10600-10605.	5.6	63
12	Formation of Highly Ordered Organic Monolayers by Dative Bonding:Â Pyridine on Ge(100). Journal of the American Chemical Society, 2003, 125, 7514-7515.	13.7	61
13	Temperature-Dependent and Gate-Tunable Rectification in a Black Phosphorus/WS <sub>2</sub> van der Waals Heterojunction Diode. ACS Applied Materials & Interfaces, 2018, 10, 13150-13157.	8.0	61
14	Effect of hydrogen on the surface-energy anisotropy of diamond and silicon. Physical Review B, 1998, 57, 6262-6265.	3.2	56
15	The presence of CH3NH2 neutral species in organometal halide perovskite films. Applied Physics Letters, 2016, 108, .	3.3	50
16	Controlled Electrochemical Intercalation of Graphene/ <i>h-</i> BN van der Waals Heterostructures. Nano Letters, 2018, 18, 460-466.	9.1	49
17	Electronic Properties of Bilayer Graphene Strongly Coupled to Interlayer Stacking and an External Electric Field. Physical Review Letters, 2015, 115, 015502.	7.8	47
18	Surface Instability of Sn-Based Hybrid Perovskite Thin Film, CH <sub>3</sub> NH <sub>3</sub> SnI <sub>3</sub> : The Origin of Its Material Instability. Journal of Physical Chemistry Letters, 2018, 9, 2293-2297.	4.6	45

#	Article	IF	CITATIONS
19	Van der Waals density functional theory study for bulk solids with BCC, FCC, and diamond structures. Current Applied Physics, 2015, 15, 885-891.	2.4	43
20	Crystal Shape of a Nickel Particle Related to Carbon Nanotube Growth. Japanese Journal of Applied Physics, 2002, 41, 6142-6144.	1.5	41
21	Double Dative Bond Configuration:Â Pyrimidine on Ge(100). Journal of Physical Chemistry B, 2005, 109, 348-351.	2.6	40
22	Indirect-direct band gap transition through electric tuning in bilayer MoS2. Journal of Chemical Physics, 2014, 140, 174707.	3.0	40
23	Reduction of Fermi level pinning at Au–MoS <sub>2</sub> interfaces by atomic passivation on Au surface. 2D Materials, 2017, 4, 015019.	4.4	40
24	Electronic structure calculations of metal-nanotube contacts with or without oxygen adsorption. Physical Review B, 2005, 72, .	3.2	39
25	Theoretical study of hydrogen-covered diamond (100) surfaces: A chemical-potential analysis. Physical Review B, 1997, 55, 9975-9982.	3.2	38
26	Dissociative Chemisorption of Methanol on Ge(100). Journal of Physical Chemistry C, 2007, 111, 15013-15019.	3.1	37
27	One-dimensional hexagonal boron nitride conducting channel. Science Advances, 2020, 6, eaay4958.	10.3	37
28	Effect of Annealing in Ar/H <sub>2</sub> Environment on Chemical Vapor Deposition-Grown Graphene Transferred With Poly (Methyl Methacrylate). IEEE Nanotechnology Magazine, 2015, 14, 70-74.	2.0	34
29	Band Alignment at Au/MoS <sub>2</sub> Contacts: Thickness Dependence of Exfoliated Flakes. Journal of Physical Chemistry C, 2017, 121, 22517-22522.	3.1	34
30	Remote homoepitaxy of ZnO microrods across graphene layers. Nanoscale, 2018, 10, 22970-22980.	5.6	33
31	High-throughput screening of metal-porphyrin-like graphenes for selective capture of carbon dioxide. Scientific Reports, 2016, 6, 21788.	3.3	31
32	Black Phosphorus-IGZO van der Waals Diode with Low-Resistivity Metal Contacts. ACS Applied Materials & Interfaces, 2019, 11, 10959-10966.	8.0	31
33	Monolithic Interface Contact Engineering to Boost Optoelectronic Performances of 2D Semiconductor Photovoltaic Heterojunctions. Nano Letters, 2020, 20, 2443-2451.	9.1	31
34	Atomic and Electronic Structure of Pyridine on Ge(100). Journal of Physical Chemistry B, 2004, 108, 15229-15232.	2.6	30
35	Remote heteroepitaxy across graphene: Hydrothermal growth of vertical ZnO microrods on graphene-coated GaN substrate. Applied Physics Letters, 2018, 113, .	3.3	30
36	Phase stability of transition metal dichalcogenide by competing ligand field stabilization and charge density wave. 2D Materials, 2015, 2, 035019.	4.4	29

#	Article	IF	CITATIONS
37	Ferromagnetic contact between Ni and MoX <sub>2</sub> (X  =  S, Se, or Te) with Fermi-leve Materials, 2017, 4, 024006.	el pinning. 4.4	2D <sub>28</sub>
38	Realistic adsorption geometries and binding affinities of metal nanoparticles onto the surface of carbon nanotubes. Applied Physics Letters, 2009, 94, .	3.3	27
39	First-principles study of carbon atoms adsorbed on MgO(100) related to graphene growth. Current Applied Physics, 2013, 13, 327-330.	2.4	27
40	Elastic properties and stacking fault energies of Cr2Ta. Intermetallics, 1999, 7, 1169-1172.	3.9	26
41	Surface energy anisotropy of iron surfaces by carbon adsorption. Current Applied Physics, 2003, 3, 457-460.	2.4	26
42	Ab initio study of adsorption properties of hazardous organic molecules on graphene: Phenol, phenyl azide, and phenylnitrene. Chemical Physics Letters, 2015, 618, 57-62.	2.6	26
43	Significant THz absorption in CH3NH2 molecular defect-incorporated organic-inorganic hybrid perovskite thin film. Scientific Reports, 2019, 9, 5811.	3.3	26
44	Thicknessâ€Dependent, Gateâ€Tunable Rectification and Highly Sensitive Photovoltaic Behavior of Heterostructured GeSe/WS <sub>2</sub> p–n Diode. Advanced Materials Interfaces, 2020, 7, 2000893.	3.7	25
45	Selective-Area Remote Epitaxy of ZnO Microrods Using Multilayer–Monolayer-Patterned Graphene for Transferable and Flexible Device Fabrications. ACS Applied Nano Materials, 2020, 3, 8920-8930.	5.0	25
46	Theoretical study on cracking behavior in two-phase alloys Cr–Cr2X (X=Hf, Nb, Ta, Zr). Intermetallics, 2001, 9, 799-805.	3.9	24
47	Study of Adsorption and Decomposition of H2O on Ge(100). Journal of Physical Chemistry B, 2005, 109, 24445-24449.	2.6	24
48	Bidentate Structures of Acetic Acid on Ge(100):  The Role of Carboxyl Oxygen. Journal of Physical Chemistry C, 2007, 111, 5941-5945.	3.1	23
49	Graphitic Carbon Growth on MgO(100) by Molecular Beam Epitaxy. Journal of Physical Chemistry C, 2012, 116, 7380-7385.	3.1	23
50	Investigations of Vacancy Structures Related to Their Growth in h-BN Sheet. Nanoscale Research Letters, 2017, 12, 445.	5.7	23
51	Tailoring Surface Properties via Functionalized Hydrofluorinated Graphene Compounds. Advanced Materials, 2019, 31, e1903424.	21.0	23
52	Rapid synthesis of graphene by chemical vapor deposition using liquefied petroleum gas as precursor. Carbon, 2019, 145, 462-469.	10.3	23
53	Carbon diffusion around the edge region of nickel nanoparticles. Applied Physics Letters, 2008, 92, 043103.	3.3	22
54	Atomic and electronic structure of methanol on Ge(100). Surface Science, 2010, 604, 129-135.	1.9	22

#	Article	IF	CITATIONS
55	Van der Waals heterojunction diode composed of WS <sub>2</sub> flake placed on p-type Si substrate. Nanotechnology, 2018, 29, 045201.	2.6	21
56	In-Depth Structural Characterization of 1T-VSe <sub>2</sub> Single Crystals Grown by Chemical Vapor Transport. Crystal Growth and Design, 2020, 20, 2860-2865.	3.0	21
57	Role of hydrogen inSiH2adsorption on Si(100). Physical Review B, 1998, 58, R13363-R13366.	3.2	20
58	Hydrogen adsorption on hexagonal silicon nanotubes. Solid State Communications, 2008, 148, 469-471.	1.9	20
59	First-principles study of substitutional carbon pair and Stone–Wales defect complexes in boron nitride nanotubes. Chemical Physics Letters, 2012, 522, 79-82.	2.6	20
60	Atomic and electronic structure of acetic acid on Ge(100). Surface Science, 2006, 600, 3629-3632.	1.9	19
61	Energy Bandgap and Edge States in an Epitaxially Grown Graphene/h-BN Heterostructure. Scientific Reports, 2016, 6, 31160.	3.3	19
62	Ab initio study of adsorption behaviors of molecular adsorbates on the surface and at the edge of MoS 2. Current Applied Physics, 2018, 18, 1013-1019.	2.4	18
63	Ab initio Calculations with van der Waals Corrections: Benzene-benzene Intermolecular Case and Graphite. Journal of the Korean Physical Society, 2011, 59, 196-199.	0.7	18
64	Atomic and Electronic Structure of Pyrrole on Ge(100). Journal of Physical Chemistry C, 2008, 112, 7412-7419.	3.1	17
65	Ab-initio Study of Interactions of Gold Atoms with Hydroxylated MgO(001) Surfaces. Journal of the Physical Society of Japan, 2012, 81, 054601.	1.6	17
66	Adsorption and Surface Diffusion of Pt Atoms on Hydroxylated MgO(001) Surfaces. Journal of the Physical Society of Japan, 2013, 82, 034603.	1.6	16
67	Hydrogen-Bonded Amino Acid Network of Histidine on Ge(100). Journal of Physical Chemistry C, 2011, 115, 4636-4641.	3.1	15
68	Metallization of the semiconducting carbon nanotube by encapsulated bromine molecules. Physica E: Low-Dimensional Systems and Nanostructures, 2005, 29, 693-697.	2.7	14
69	Van der Waals Density Functional Theory Study of Molecular Adsorbates on MoX2(X = S, Se or Te). Journal of the Korean Physical Society, 2018, 73, 100-104.	0.7	14
70	3D graphene-cellulose nanofiber hybrid scaffolds for cortical reconstruction in brain injuries. 2D Materials, 2019, 6, 045043.	4.4	14
71	First-principles calculation of stacking fault and twin boundary energies of Cr2Nb. Philosophical Magazine A: Physics of Condensed Matter, Structure, Defects and Mechanical Properties, 2000, 80, 871-880.	0.6	13
72	Chemical Reactions and Adsorption Geometries of Pyrrole on Ge(100). Journal of Physical Chemistry B, 2006, 110, 7938-7943.	2.6	13

#	Article	IF	CITATIONS
73	Polar oxide substrates for graphene growth: A first-principles investigation of graphene on MgO(111). Current Applied Physics, 2013, 13, 803-807.	2.4	13
74	Conserving approximations: Electron gas with exchange effects. Physical Review B, 1994, 50, 8182-8188.	3.2	12
75	Adsorption Structure and Reaction Mechanism of Purine on Ge(100) Studied by Scanning Tunneling Microscopy and Theoretical Calculations. Journal of Physical Chemistry C, 2012, 116, 6953-6959.	3.1	12
76	Point defects in turbostratic stacked bilayer graphene. Nanoscale, 2017, 9, 13725-13730.	5.6	12
77	Investigation of atomic and electronic properties of 2D-MoS <sub>2</sub> /3D-GaN mixed-dimensional heterostructures. Nanotechnology, 2019, 30, 404002.	2.6	12
78	Enhanced binding strength between metal nanoclusters and carbon nanotubes with an atomic nickel defect. Nanotechnology, 2012, 23, 205204.	2.6	11
79	<i>In Situ</i> Atomic Level Dynamics of Heterogeneous Nucleation and Growth of Graphene from Inorganic Nanoparticle Seeds. ACS Nano, 2016, 10, 9397-9410.	14.6	11
80	Discrimination of Chiral Adsorption Configurations: Styrene on Germanium(100). Journal of Physical Chemistry C, 2009, 113, 1426-1432.	3.1	10
81	Thermally Induced Desulfurization: Structural Transformation of Thiophene on the Si(100) Surface. Journal of Physical Chemistry C, 2013, 117, 11731-11737.	3.1	9
82	Theoretical Demonstration of the Ionic Barristor. Nano Letters, 2016, 16, 2090-2095.	9.1	9
83	Understanding filamentary growth and rupture by Ag ion migration through single-crystalline 2D layered CrPS4. NPG Asia Materials, 2020, 12, .	7.9	9
84	Temperature dependence of the Hartree-Fock approximation. Physical Review B, 1994, 50, 7284-7290.	3.2	8
85	Thermodynamic design of a high temperature chemical vapor deposition process to synthesize α-SiC in Si-C-H and Si-C-H-Cl systems. Journal of Crystal Growth, 2018, 485, 78-85.	1.5	8
86	Substrate effect on doping and degradation of graphene. Carbon, 2021, 184, 651-658.	10.3	8
87	Temperature dependence of the Hartree-Fock approximation in two dimensions. Physical Review B, 1995, 52, 7860-7863.	3.2	7
88	Energetics of the dihydride phases on the diamond (100) surface. Physical Review B, 2002, 65, .	3.2	7
89	Theoretical STM images of alkaline-earth metal adsorbed Si(111)3×2 surfaces. Surface Science, 2006, 600, 3606-3609.	1.9	7
90	Graphene oxide catalyzed cis-trans isomerization of azobenzene. APL Materials, 2014, 2, .	5.1	7

#	Article	IF	CITATIONS
91	Mixed-dimensional 2D/3D heterojunctions between MoS <sub>2</sub> and Si(100). Physical Chemistry Chemical Physics, 2018, 20, 25240-25245.	2.8	7
92	First-Principles Study of Atomic and Electronic Structure of Ba/Si(111). Journal of the Physical Society of Japan, 2002, 71, 2761-2764.	1.6	6
93	Effect of Hydrogen on Carbon Diffusion on Ni(111). Japanese Journal of Applied Physics, 2004, 43, 773-774.	1.5	6
94	Origins of dihydrogen binding to metal-inserted porphyrins: Electric polarization and Kubas interaction. Journal of Chemical Physics, 2011, 134, 234701.	3.0	6
95	Doping effect in graphene on oxide substrates: MgO(111) and SiO2(0001). Current Applied Physics, 2015, 15, S103-S107.	2.4	6
96	Rapid chemical vapor deposition of graphene using methanol as a precursor. Carbon Letters, 2021, 31, 307-313.	5.9	6
97	Ab initio study of hydrogen binding on Ca-inserted porphyrin. Vacuum, 2009, 84, 537-539.	3.5	5
98	Effect of charge-transfer complex on the energy level alignment between graphene and organic molecules. Applied Physics Letters, 2012, 100, 183102.	3.3	5
99	Strain-induced non-linear optical characteristics of pyroelectric PbVO_3 epitaxial thin films. Optical Materials Express, 2017, 7, 62.	3.0	5
100	Effect of atomic passivation at Ni-MoS2 interfaces on contact behaviors. Current Applied Physics, 2020, 20, 132-136.	2.4	5
101	Transport gaps in ideal zigzag-edge graphene nanoribbons with chemical edge disorder. Applied Surface Science, 2020, 512, 144714.	6.1	5
102	Electronic structure of graphene/Y2C heterostructure and related doping effect. Current Applied Physics, 2021, 28, 13-18.	2.4	5
103	Correlation energy and its temperature dependence. Physical Review B, 1996, 53, 1215-1224.	3.2	4
104	Monovacancy and substitutional defects in hexagonal silicon nanotubes. Solid State Communications, 2009, 149, 408-411.	1.9	4
105	Enhanced Deseleniumization of Selenophene Molecules Adsorbed on Si(100)-2 × 1 Surface. Journal of Physical Chemistry C, 2011, 115, 17856-17860.	3.1	4
106	A first-principles study on the adsorption of ethylenediamine on Ge(100). Physical Chemistry Chemical Physics, 2017, 19, 16881-16887.	2.8	4
107	Spin-polarized Hartree-Fock approximation at nonzero temperatures. Physical Review B, 1995, 51, 17417-17430.	3.2	3
108	Atomic and electronic structure of styrene on Ge(100). Surface Science, 2011, 605, 1438-1444.	1.9	3

#	Article	IF	CITATIONS
109	Observation of graphene grain boundaries through selective adsorption of rhodamine B using fluorescence microscopy. Carbon, 2016, 108, 72-78.	10.3	3
110	Adsorption of Acetonitrile on Si(111)-(7 $ ilde{A}$ — 7). ACS Omega, 2020, 5, 24179-24185.	3.5	3
111	Contact properties of 2D/3D GaSe/Si(1Â1Â1) heterostructure. Applied Surface Science, 2020, 516, 145969.	6.1	3
112	Structure of Pyrrole on Ge(100). Japanese Journal of Applied Physics, 2006, 45, 2148-2150.	1.5	2
113	Structure of Clycine on Ge(100): Ab Initio Study of Its Scanning Tunneling Microscopy Images. Journal of Physical Chemistry C, 2012, 116, 13890-13895.	3.1	2
114	Ab initio Investigations of Carbon Atoms Adsorbed on α-Al2O3 Surfaces in Relation to Graphene Growth. Journal of the Physical Society of Japan, 2013, 82, 114709.	1.6	2
115	Edge-functionalization of armchair graphene nanoribbons with pentagonal-hexagonal edge structures. Journal of Physics Condensed Matter, 2017, 29, 245301.	1.8	2
116	Functionalization of Ge(1†0†0) surface by adsorption of phenylthiol. Applied Surface Science, 2018, 456, 908-914.	6.1	2
117	Effects of intercalated atoms on electronic structure of graphene nanoribbon/hexagonal boron nitride stacked layer. Scientific Reports, 2019, 9, 3623.	3.3	2
118	Layer dependent electrical transport in exfoliated graphene FETs under UV illumination. Applied Surface Science, 2019, 479, 863-873.	6.1	2
119	Effect of Point Defects on Electronic Structure of Monolayer GeS. Nanomaterials, 2021, 11, 2960.	4.1	2
120	Spatial variation in the electronic structures of carpetlike graphene nanoribbons and sheets. Current Applied Physics, 2014, 14, 1687-1691.	2.4	1
121	Indium-contacted van der Waals gap tunneling spectroscopy for van der Waals layered materials. Scientific Reports, 2021, 11, 17790.	3.3	1